Structural and optical properties of 3D growth multilayer InGaN/GaN quantum dots by metalorganic chemical vapor deposition

ARTICLE *in* JOURNAL OF CRYSTAL GROWTH · JUNE 2004

Impact Factor: 1.7 · DOI: 10.1016/j.jcrysgro.2004.02.108

Available online at www.sciencedirect.com
SCIENCE DIRECT®
Journal of Crystal Growth 266 (2004) 423–428
JOURNAL OF CRYSTAL GROWTH
www.elsevier.com/locate/jcrysgro

Structural and optical properties of 3D growth multilayer InGaN/GaN quantum dots by metalorganic chemical vapor deposition

Xiuxun Han*, Zhen Chen, Dabing Li, Jiejun Wu, Jiemin Li, Xuehao Sun, Xianglin Liu, Peide Han, Xiaohui Wang, Qinsheng Zhu, Zhanguo Wang

Key Laboratory of Semiconductor Materials Science, Institute of Semiconductors, Chinese Academy of Sciences, P.O. Box 912, Beijing 100083, People's Republic of China

Received 8 January 2004; accepted 20 February 2004
Communicated by M. Schieber

Abstract

Multilayer InGaN/GaN quantum dots (QDs) were grown on sapphire substrates through a three-dimensional growth mode, which was initiated by a special passivation processing introduced into the normal growth procedure. Surface morphology and photoluminescence properties of QDs with different stacking periods (from one to four) were investigated. The temperature dependences of the PL peak energies were found to show a great difference between two-layer and three-layer QDs. The fast redshift and the reversed sigmoidal temperature dependences of the PL energies for the former were attributed to the thermally activated carrier transfer from small to large dots. However, the increase of both the dot size and the spatial space among dots with the growing stacking periods reduced the carrier escape and retrapping.

PACS: 78.55.Cr; 78.67.Hc; 81.05.Ea; 81.07.Ta; 81.15.Gh

Keywords: A1. Nanostructure; A1. Optical microscopy; A3. Metalorganic vapor phase epitaxy; B1. Nitrides

1. Introduction

In response to the requirements of high performance optoelectronic devices, an increasing interest has been attracted in the fabrication of GaN-based low-dimensional structures [1–3]. Especially, as a normally used active layer in existing light emitting diodes (LEDs) and laserdiodes (LDs), InGaN bears numerous investigations to understand its basic optical properties. It has been argued that the enhanced photoluminescence (PL) intensity originates from excitons localized in In-riched regions of the well, which act as self-assembled quantum dots and localize the carriers to hinder their migration toward nonradiative centers [4–7]. Thus, it can be expected that using InGaN quantum dots structures as the active layer will lead to much lower threshold currents and narrower emission spectra. Some good work is on the way in proving these

*Corresponding author. Tel./fax: +86-10-8230-4968.
E-mail address: xxhan@red.semi.ac.cn (X. Han).

0022-0248/$ - see front matter © 2004 Elsevier B.V. All rights reserved.
doi:10.1016/j.jcrysgro.2004.02.108

predictions, and a room-temperature lasing oscillation in a laser structure with InGaN QDs embedded into the active layer has been observed [8]. Besides the commonly adopted methods including self-organization [9], which is characterized by Stranski–Krastanow (S–K) growth mode, anti-surfactant (e.g. silicon)-assisted growth [10], selective growth [11], and several new methods emerged recently to obtain InGaN QDs. Oliver et al. [12] annealed a thin InGaN epilayer grown on a GaN buffer layer at the growth temperature in molecular nitrogen and induced quantum dot formation. Ji and coworkers [13] also fabricated nanoscale InGaN QDs by inserting an interrupted growth mode (12 s) during the deposition of 9 MLs InGaN. Although much progress has been made, fabrication of size and uniform distribution controlled InGaN QDs still remains as great challenges in these methods mentioned above. The fluctuation in dot size and indium composition will broaden quantized energy levels and destroy the unique properties expressed by single QD, which makes it more difficult to understand the InGaN QD's detailed emission mechanism. Random distribution of each QD may damage the coherence of the optical and electronic wave propagating through the system [3]. Together with the usually low density, these factors are now blocking the way to realize their predicted potential application in device fabrication. Due to the lack of in situ detecting technology, these problems are more prominent in the metalorganic chemical vapor deposition (MOCVD) system compared with molecular beam epitaxy. Further research work is still in urgent requirement.

In this paper, we used our recently developed method and obtained stacked InGaN QDs, which is characterized by introducing a passivation processing in growth procedure. Atomic force microscope (AFM) measurement results of first layer QDs evidenced its high density. Detailed optical properties of different layer QDs are also presented.

2. Experiment details

The samples were grown on the sapphire (0 0 0 1) substrates in a horizontal, low-pressure MOCVD system. Trimethylgallium (TMG), Ethyldimethylindium (EDMIn) were used as group III sources, NH_3 as group V sources, and H_2, N_2 as carried gases, respectively. After a 1-μm-thick high-temperature GaN (HT-GaN) was grown at 1030°C by a regular three-step process [14], the substrate (HT-GaN) was taken out of the reacting chamber and exposed in the atmosphere for 24 h to obtain the passivated surface. Then it was transferred back into the reactor chamber after performing following sequential cleaning steps: ultrasonic cleaning by acetone and ethanol, being etched in HNO_3:H_2SO_4 (1:1) solution, and rinsed in de-ionized water. The passivated substrate was heated to 550°C and hold for about 20 min in an H_2 ambient. A GaN seeding layer was deposited at 550°C. Then the temperature was raised to 850°C. The carried gas changed to N_2, and InGaN QDs with the height of about 15 nm formed on the GaN seeding layer after a short supply of TMG and EDMIn. Thus, the growth of monolayer InGaN QDs sample was completed. For the samples containing two, three, and four periods of InGaN QDs, the same experiment parameters were used except that 15 nm-thick GaN spacer layers were inserted. During the growth, the flow rate of TMG was 25 μmol/min, and that of NH_3 was 3 standard liters per minute (SLM) with carried gases of 3 SLM for H_2 and 4 SLM for N_2. More details of the growth experiment were described elsewhere [15].

The AFM was used to observe the surface morphology. PL experiment was carried out using a 325-nm line of a Kimmon He-Cd laser with an exciting power of 25 mW.

3. Results and discussion

Fig. 1 illustrates the surface morphology of the InGaN QDs with stacking layers ranging from one to four. It can be seen from Fig. 1(a), the morphology of the first layer, that a relatively high dot density of $8 \times 10^{10}\,cm^{-2}$ can be obtained. The dot height and width is about 15 and 30 nm, respectively, which evidences that the passivation growth provides another efficient way to get QDs. The growth mechanism is expected to be like this. First, the active growth is broken when HT-GaN

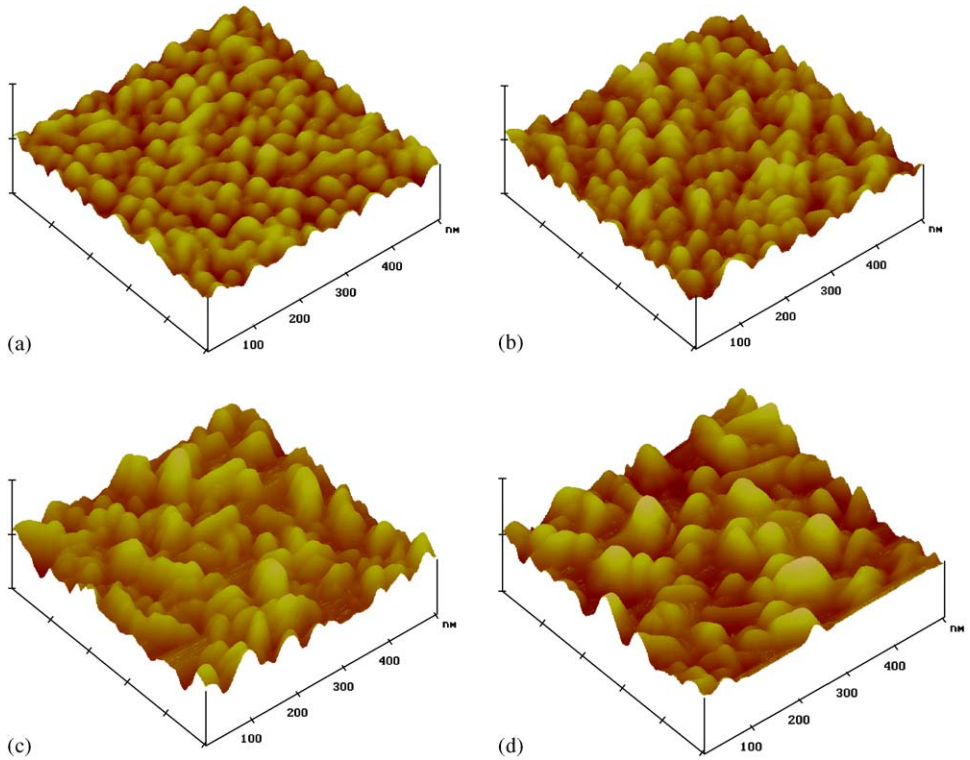

Fig. 1. AFM morphology of the InGaN/GaN QDs with (a) monolayer, (b) two-layer, (c) three-layer, and (d) four-layer.

layer growth is finished and the temperature decreases to room temperature. After the exposure in the air for about 24 h, the surface energy changes significantly, and the increasing barrier energy will hinder the adatom's sufficient migration. Additionally, the relatively low growth temperature of oncoming GaN seeding layer will enhance the 3D growth model. Second, compared with uninterrupted growth, exposure in the air will induce surface contamination to a certain extent, though cleaning and etching steps has been followed. These impurities on the substrate surface can act as a nucleation center for the 3D crystal growth, which has been observed in other material growth system [16]. Hence, these two factors lead to the formation of dot-like GaN seeding layer, which is believed to play the key role to the form of InGaN QDs. This mechanism also well explains why our QD's size is a little bigger than other researcher's results, e.g. by self-organization methods. Continuing 3D growth from GaN seeding layer to InGaN dots is its origin. Through adjusting growth time of seeding layer, small size dots may be achieved; so further optimization of the growth parameters is still needed.

Another phenomenon illustrated in Fig. 1 is that the dot size tends to increase, but the density tends to decrease with the rising of stacked layer numbers. Moreover, as the stacking periods increases, overlapped dots gradually changed to rather isolated ones. We have attributed the phenomena to the strain concerned memory effects that the buried dots exert on the top ones [17].

Accordingly, the 5 K PL spectra of samples consisting one to four layers of InGaN/GaN QDs show significant differences in Fig. 2. An apparent red shift of peak energy attributed to the InGaN QDs emission can be seen, changing from 3.325 to 3.264 eV. A large shift takes place between two- and three-layer QDs. This red shift is interpreted as that the increasing size of QDs reduces the quantum confinement effect. For three- and four-

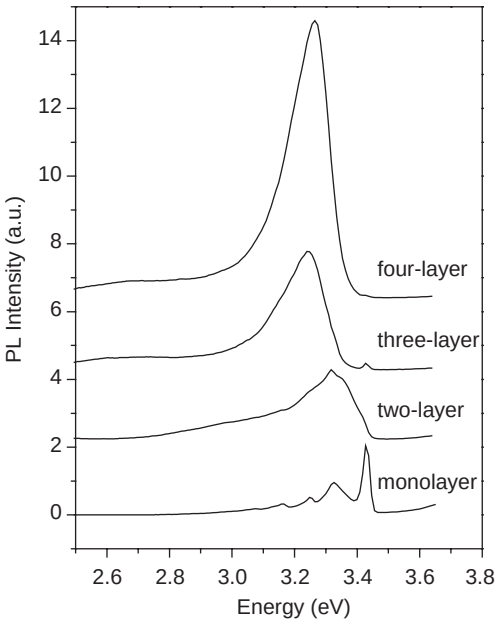

Fig. 2. PL spectra of InGaN/GaN QDs with different stacking layers at 5 K.

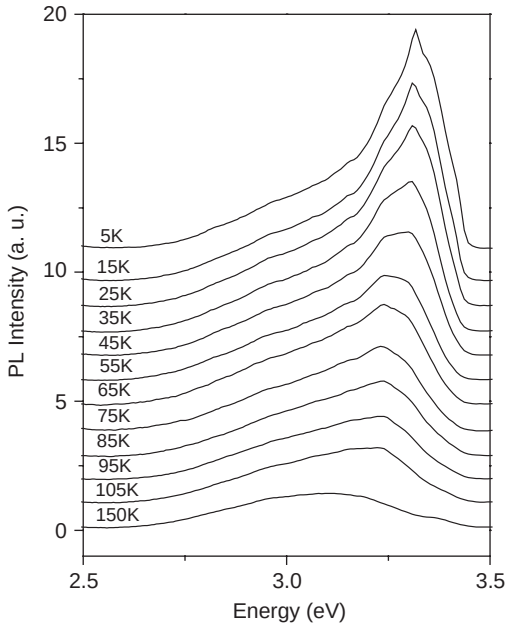

Fig. 3. PL spectra of tow-layer InGaN/GaN QDs in temperature range from 5 to 150 K.

layer QDs, average size does not differ so much, and the energy shift is thus small. Additionally, an increase of quantum confined Stark effect also strengthens this shift further. The emission intensity also enlarges greatly from one- to four-layer QDs. Even if just comparing two-layer QDs from the monolayer ones, emission intensity increases about 10 times and that enlargement is believed to benefit a lot from the increasing collected QDs numbers. Note that the temperature we used to grow InGaN is a little higher, which results in the relatively low component of indium and large emission energies exhibited in the PL spectra. The peak located at 3.427 eV for monolayer QDs is attributed to the bound exciton recombination of GaN, coming from the underlying GaN seeding layer or the HT-GaN substrate. With the increasing of stacking layers, it reduces its density and disappears in the end. The emerged two peaks on the low-energy side for the monolayer QDs (0.071 and 0.145 eV lower than 3.325 eV, respectively) are attributed to the TO phonon replica of InGaN QDs [19]. With the increase of stacking layers, their signals immerge into the strong and broadened peak of InGaN QDs induced by the fluctuation in size.

PL measurements were carried out at different temperatures in order to investigate the temperature dependences of peak energies for InGaN QDs assembly with different sizes. Figs. 3 and 4 show the results. For two-layer InGaN QDs (see Fig. 3), the dominant peak energy shows a fast red shift when the temperature rises from 5 to 150 K. Furthermore, when the temperature changes from 35 to 65 K, the dominating status shows an obvious exchange between two Gaussian peaks which can be decomposed from the main emission peak. The higher energy governs the low-temperature range, while the lower one masters the high-temperature range. For three-layer QDs (see Fig. 4), however, this does not hold good. Although a red shift is also evident, but it does not change so fast, and no obvious exchange of dominating status between two peaks is found. For the convenience of such a feature's confirmation, Figs. 5(a) and (b) show the temperature dependencies of the peak energies for two- and three-layer InGaN QDs, respectively. In Fig. 5(a), the so-called reversed sigmoidal temperature

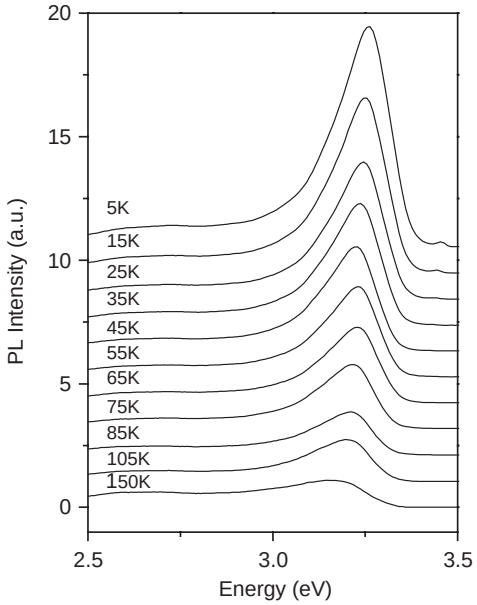

Fig. 4. PL spectra of three-layer InGaN/GaN QDs in temperature range from 5 to 150 K.

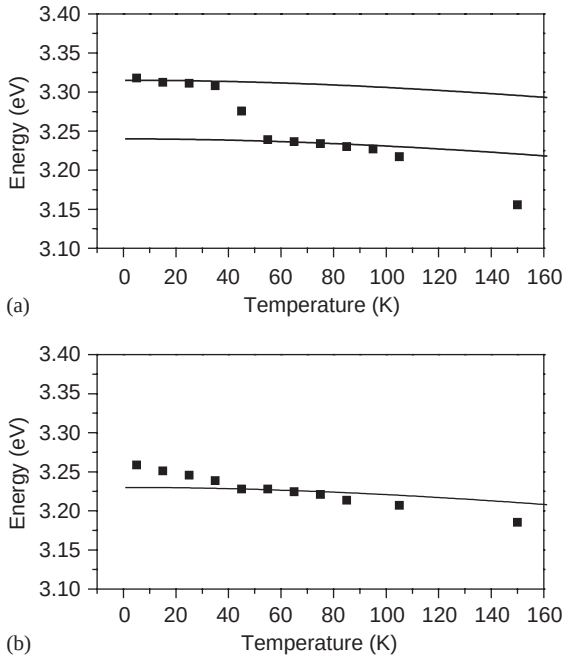

Fig. 5. Temperature dependences of the PL peak energies for two-layer (a) and three-layer (b) InGaN/GaN QDs (closed squares). The lines are calculated using the Varshni law with different parameters concerning GaN.

dependence of PL spectra can be seen; but in Fig. 5(b), the temperature dependence changes more moderately. The continuous line in Fig. 5 are calculated according to Varshni law $E_g(T) = E(0) - \alpha T^2/(\beta + T)$ with parameters of GaN [17]. The fact that two different lines are needed to fit two different temperature ranges in Fig. 5(a) implies that the dot assembly consists of different dot families. In our case, the most obvious factor is the dot size. Adequate proof can be found from the AFM morphology of two-layer QDs (see Fig. 1(b)). Big dots with average diameter of about 35 nm and small ones with average diameter of 20 nm are overlapped together. Their respective densities are comparable. As temperature increases, the localized carriers will be released, and penetration of the wave functions of carriers in coupled QDs will be enhanced. It has been illustrated that the higher activation energy corresponds to the QDs with smaller peak energies [18]. In other words, the carriers with deeper localized energies in small dots prefer to escape into lower confined states of large dots. Thus, when the temperature reaches a finite range, 35–55 K for two-layer QDs, electrons localized in small dots may overcome the barrier and transfer to the big dots due to thermal activation before radiative recombination occurs. Hence, the reason why the exchange of dominating status happens lies in the fact that the small dots with high energies dominate the PL spectra at low temperatures, and big dots with low energies dominate the PL spectra at high one. This mechanism has been well explained for InAs quantum dots by Brusaferri and coworkers [18].

For three-layer QDs (see Fig. 5(b)), the transfer of carriers is hardly observed. The reason also can be explained from the AFM morphology. In Fig. 1(c) big dots nearly reach their overwhelming stations. The space among dots is large compared with two-layer QDs, which makes it difficult to realize efficient transfer between dots. Thus no obvious reversed sigmoidal temperature dependences of PL spectra can be seen. It is worth noting that one-parameter Varshni law cannot fit this dependence well. It is possibly due to the collective effects coming from the two underlying layers of

QDs and also a small number of small QDs in its own layer. The total number of QDs and the fluctuation of sizes are both enlarged when another layer is added to the two-layer one. The combination of their different peak positions leads to the formation of a broad dominating peak, and hence a deviation from one-parameter Varshni law.

4. Conclusions

A passivation processing was used to obtain the multilayer InGaN/GaN QDs by MOCVD. The 3D growth mode is expected to take place. With the increase of stacking layers, the dot size tends to increase, and the space among dots tends to enlarge, which induces different temperature dependence behaviors of PL peak energy for different stacked layers. Thermally activated excitation transfer between small and big QDs accounts for the reversed sigmoidal temperature dependences of PL spectra for two-layer QDs. However, for three-layer ones, which are characterized by the distribution of both big and rather isolated QDs, such a transfer phenomenon is not so obvious.

Acknowledgements

This work is financially supported by the National Natural Science Foundation of China (Nos. 60136020 and 60086001) and the Special Funds for Major State Basic Research Project under Contract No. G20000683.

References

[1] S. Nakamura, T. Mukai, M. Senoh, Appl. Phys. Lett. 64 (1994) 1687.
[2] S. Nakamura, M. Senoh, S. Nagahama, N. Iwasa, T. Yamada, T. Matsushita, H. Kiyoku, Y. Sugimoto, Appl. Phys. Lett. 68 (1996) 3269.
[3] D. Ming, M.A. Reshchikov, H. Morkoç, Int. J. High Speed Electron. Systems. 12 (2002) 79.
[4] R.W. Martin, P.G. Middleton, K.P. O'Donnell, W. Van der Stricht, Appl. Phys. Lett. 74 (1999) 263.
[5] L. Nistor, H. Bender, A. Vantomme, M.F. Wu, J. Van Landuyt, K.P. O'Donnell, R. Martin, K. Jacobs, I. Moerman, Appl. Phys. Lett. 77 (2000) 507.
[6] P. Riblet, H. Hirayama, A. Kinoshita, A. Hirata, T. Sugano, Y. Aoyagi, Appl. Phys. Lett. 75 (1999) 2241.
[7] I.L. Krestnikov, N.N. Ledentsov, A. Hoffmann, D. Bimberg, A.V. Sakharov, W.V. Lundin, A.F. Tsatsul'nikov, A.S. Usikov, Zh.I. Alferov, Yu.G. Musikhin, D. Gerthsen, Phys. Rev. B 66 (2002) 155310.
[8] K. Tachibana, T. Someya, Y. Arakawa, IEEE J. Sel. Top. Quantum Electron. 6 (2000) 475.
[9] O. Moriwaki, T. Someya, K. Tachibana, S. Ishida, Y. Arakawa, Appl. Phys. Lett. 76 (2000) 2361.
[10] S. Tanaka, S. Iwai, Y. Aoyagi, Appl. Phys. Lett. 69 (1996) 4096.
[11] D. Kapolnek, S. Keller, R.D. Underwood, S.P. DenBaars, U.K. Mishra, J. Crystal Growth 189 (1998) 83.
[12] R.A. Oliver, G. Andrew, D. Briggs, M.J. Kappers, C.J. Humphreys, S. Yasin, J.H. Rice, J.D. Smith, R.A. Taylor, Appl. Phys. Lett. 83 (2003) 755.
[13] L.W. Ji, Y.K. Su, S.J. Chang, L.W. Wu, T.H. Fang, J.F. Chen, T.Y. Tsai, Q.K. Xue, S.C. Chen, J. Crystal Growth 249 (2003) 144.
[14] H. Amano, N. Sawaki, I. Akasaki, Y. Toyoda, Appl. Phys. Lett. 48 (1986) 353.
[15] Z. Chen, D. Lu, P. Han, X. Liu, X. Wang, Y. Li, H. Yuan, Y. Lu, D. Li, Q. Zhu, Z. Wang, X. Wang, L. Yan, J. Crystal Growth 243 (2002) 19.
[16] Y. Gotoh, S. Ino, H. Komatsu, J. Crystal Growth 56 (1982) 498.
[17] H. Morkoç, Nitride Semiconductors and Devices, Springer, Heidelberg, Germany, 1999.
[18] L. Brusaferri, S. Sanguinetti, E. Grilli, M. Guzzi, A. Bignazzi, F. Bogani, L. Carraresi, M. Colocci, A. Bosacchi, P. Frigeri, S. Franchi, Appl. Phys. Lett. 69 (1996) 3354.
[19] Z. Chen, D. Lu, X. Liu, X. Wang, P. Han, D. Wang, H. Yuan, Z. Wang, G. Li, Z. Fang, J. Appl. Phys. 93 (2003) 316.